



1 **Critical Evaluation of Strong Ground Motions in Izmir and Implications for Future Earthquake Simulation**

2 **Results**

3 Sahin Caglar Tuna

4 Ass. Prof. Dr.; Yasar University, Izmir

5 **ABSTRACT**

6 Izmir, a major city in western Turkey, is located in a highly seismic region, subject to frequent earthquakes due to
7 its proximity to active fault systems. This paper critically evaluates the strong ground motions recorded in Izmir,
8 with a focus on understanding the implications for urban infrastructure and future seismic hazard mitigation.
9 Historically available data is collected and compared with the available ground motion prediction equations
10 (GMPE). Later, the most appropriate prediction equation is selected and used to determine the target response
11 spectrum. 2020 Sisam earthquake is a well-documented seismic event and the data from the stations are then used
12 to further calibrate the 1D site response model. Lastly, possible future events are generated and results are
13 compared with the current Turkish Earthquake Code (TEC). Amplification factors prescribed by code for İzmir
14 Bay have been surpassed by projected future events, highlighting the necessity for reassessment. Therefore, region-
15 specific seismic zoning should be established when standard code practices fall short in accounting for significant
16 site effects. Concrete recommendations about local site modification factors and evaluations on this topic have
17 been provided within the article.

18 **Keywords:** Ground motion prediction equations, Site response, Future events, Local site modification factors

19

20

21

22

23

24

25

26

27

28

29

30

31



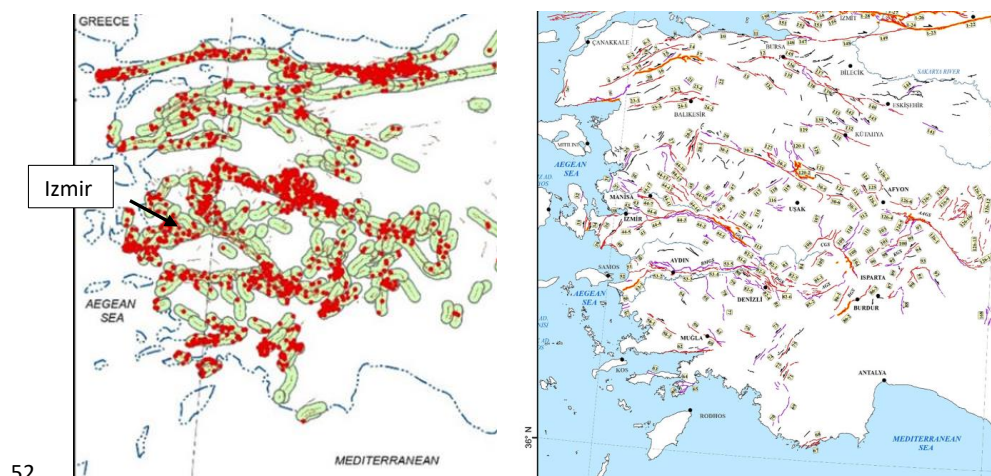
32 **1. INTRODUCTION**

33 1.1. Scope and Aim

34 Izmir, Turkey's third-largest city, is located on the Aegean coast, and its proximity to active fault lines makes it
35 highly vulnerable to seismic activity. Izmir is located within the extensional tectonic regime of the Aegean region,
36 where several active faults, including the Izmir Fault and the Seferihisar Fault, contribute to the area's high seismic
37 risk (Emre et al., 2018). The proximity of Izmir to the Hellenic subduction zone also increases its seismic hazard,
38 as this plate boundary is responsible for generating frequent and potentially large earthquakes (McKenzie, 1978).
39 In particular, shallow crustal earthquakes have historically caused significant ground shaking and damage in the
40 region (Emre et al., 2005). Some of the recent studies have detailed the active faults in the region from which, the
41 activity of the seismic hazard can be evaluated easily (Figure 1).

42 The city has been impacted by numerous destructive earthquakes throughout history. The 1688 and 1778
43 earthquakes were particularly devastating, with reports of widespread destruction (Tepe et.al. 2021). In more recent
44 times, the 2020 Samos earthquake have provided critical data on the ground motions experienced in the region.
45 These events highlighted the varying response of different local soil conditions and the importance of considering
46 site-specific factors in seismic hazard assessment (Cetin et.al, 2022).

47 Given the city's dense population and economic importance, a critical evaluation of the ground motion
48 characteristics during earthquakes is essential for improving preparedness and urban resilience. Buildings with
49 poor design or inadequate retrofitting were particularly vulnerable, as they were not able to withstand the amplified
50 seismic waves. Understanding these interactions is key to developing more effective risk mitigation strategies and
51 informing future urban planning.



53 Figure 1. Active Seismic Faults and recent earthquakes in the region (Emre et.al, 2018)

54 The purpose of this study is divided into two main parts: First part is to evaluate the strong ground motions recorded
55 in Izmir during past seismic events, particularly focusing on their effects on local geotechnical conditions and built



56 environments. In the second part, a future earthquake scenario and potential engineering outcomes will be
57 examined by using the findings obtained in the first part.

58 The steps involved in this study include:

- 59 a. Data Collection: Gathering historical earthquake data from the Izmir region, including earthquake
60 magnitudes, source-to-site distances, and PGA measurements.
- 61 b. Selection of GMPEs: Choosing GMPE models that are applicable to the regional tectonic and geological
62 conditions.
- 63 c. Comparison of GMPE Predictions and evaluation of GMPE Accuracy: Comparing the predicted PGA
64 values from different GMPEs with the observed values from historical earthquakes. Differences were
65 observed between the predicted and actual ground motions, emphasizing the importance of site-specific
66 adjustments in GMPEs for accurate seismic hazard assessment. Using statistical methods, such as Root
67 Mean Square Error (RMSE), to assess the accuracy of the GMPE predictions and identify the most
68 reliable model for the Izmir region. Apply necessary improvements for the prediction equations to comply
69 with the specific directivity and near fault effects.
- 70 d. 1D site response analysis were firstly validated with the available recordings and then set up for the future
71 earthquake scenarios.
- 72 e. Developing target spectra using the outcomes of 3rd step, evaluating future earthquakes in the region and
73 comparison with the current TEC results.
- 74 f. The study concludes with recommendations on refining seismic hazard models to account for local site
75 effects and improving the predictive accuracy of GMPEs in areas with complex soil profiles. These
76 findings have implications for earthquake-resistant design and site-specific seismic risk mitigation
77 strategies.

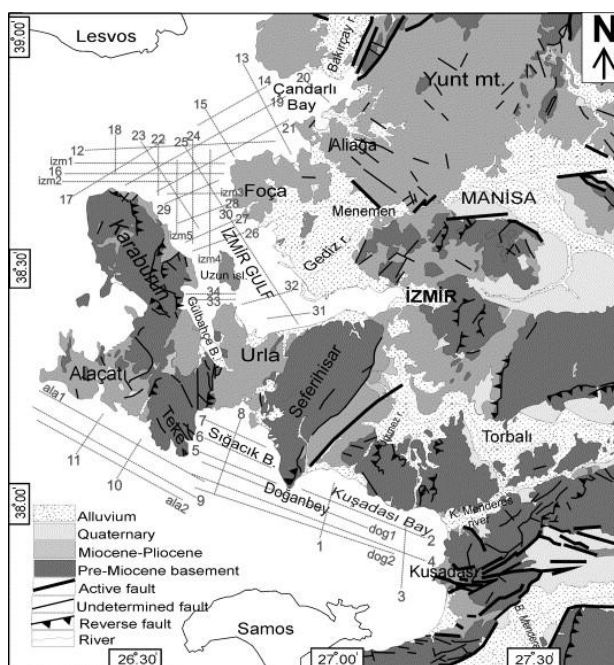
78

79 1.2. The Geological and Geotechnical Settings of Izmir Bay

80 The geological structure of Izmir is highly variable, consisting of sedimentary basins with alluvial soils and rock
81 outcrops. These heterogeneous ground conditions play a crucial role in amplifying seismic waves and influencing
82 the distribution of damage during earthquakes. This is particularly important in areas with soft soils or complex
83 geological features, which can greatly affect the intensity and frequency content of seismic waves at the surface.
84 As part of the Aegean region, Izmir is situated within an active tectonic zone characterized by extensional
85 processes and numerous fault systems, contributing to its significant seismic hazard. The Izmir Bay region is
86 located in the western part of Turkey and is part of the larger Aegean Extensional Province. This region is
87 influenced by the ongoing tectonic extension between the African and Eurasian plates, creating a highly active
88 fault system that includes both normal and strike-slip faults (Akyol et.al. 2006). The geological makeup of Izmir
89 Bay consists of a variety of rock types and sedimentary deposits that influence the behavior of seismic waves
90 during an earthquake:



- 91 • Sedimentary Basins: The region includes several sedimentary basins, including the Gediz Graben and the
92 Menderes Massif. These basins are filled with younger, unconsolidated sediments that can amplify
93 seismic waves.
94 • Alluvial Deposits: Much of the coastal region, including areas surrounding the bay, is composed of
95 alluvial deposits. These sediments, deposited by rivers, are loosely consolidated and can exacerbate
96 ground shaking during an earthquake.



97

98 Figure 2. Geology map of the study area and location of the seismic fault lines (Adapted from Ocakoglu et.al,
99 2005).

100 **2. Compilation of the strong motion dataset and predictive performance of current ground motion**
101 **models**

102 Ground Motion Prediction Equations (GMPEs) are empirical or semi-empirical mathematical models used to
103 estimate the expected level of ground shaking (ground motion) at a specific location during an earthquake. GMPEs
104 play a critical role in seismic hazard analysis and earthquake engineering by predicting key seismic parameters
105 based on several factors such as earthquake magnitude, distance to the fault, and local site conditions (Gulerce
106 et.al 2022). The Izmir region, located in Western Anatolia, is seismically active and has complex fault systems
107 and varying soil conditions. Therefore, selecting an appropriate target spectrum for this region requires a detailed
108 comparison of GMPE predictions with observed earthquake records.



109 For that aim, historical earthquake data from the Izmir region, including earthquake magnitudes, source-to-site
 110 distances, and PGA measurements were gathered. Historical ground motion records were compiled from Turkish
 111 Ministry of Interior Disaster and Emergency Management Presidency (AFAD). A total 33 earthquake events,
 112 dating from 1996 to 2024 were selected and given in Table 1 with the recorded peak ground acceleration (PGA)
 113 values. A total of 8 different GMPEs were used for comparison and validation purpose (Table 2). The predicted
 114 peak ground acceleration (PGA) values from various GMPEs with the actual observed values from historical
 115 earthquakes were compared (Figure 3).

116 Table 1. Important characteristics of the historical seismic events

Event No	Event Name	Mw	Epicentral Distance - km	Fault Mechanism	Event Depth -km	PGA Max - cm/s ²
1	10.04.2003 - Seferihisar	5.7	37.45	Strike Slip	18.7	78.57
2	17.10.2005 - Urla	5.8	58.21	Strike Slip	11	13.12
3	17.10.2005 - Urla	5.4	56.17	Strike Slip	20.5	16.51
4	20.10.2005 - Urla	5.9	58.98	Strike Slip	15.4	31.773
5	30.10.2022- Sisam	7	75.57	Normal	16.54	73.72
6	12.06.2017-Karaburun	6.2	43.87	Normal	15.86	58.306
7	11.04.2022- Buca - İzmir	4.9	9.81	Strike Slip	14.47	48.59
8	19.07.2014 - Konak- İzmir	3.7	10	Strike Slip	6.98	9.47
9	21.04.2021-Sehzadeler-Manisa	4.9	40.19	Normal	13.2	9.673
10	12.06.2017-Karaburun	6.2	89.62	Normal	15.86	25.499
11	26.06.2020- Saruhanlı-Manisa	5.5	64.1	Normal	9.29	7.109
12	8.01.2013 - Aegean Sea	6.2	194		26.83	3.642
13	24.05.2014 - Aegean Sea	6.5	255.78		25	7.659
14	02.06.2017 Ayvacik (Canakkale)	5.3	154.13	Normal	14.16	1.466
15	06.17.2017 Aegean Sea	5.3	81.15	Normal	9.11	9.42
16	07.20.2017 Aegean Sea(Bodrum)	6.5	169.93	Normal	19.44	4.44
17	18.02.2020 Kırkağaç (Manisa)	5.2	91.02	Normal	6.98	4.662
18	19.05.2011 Simav (Kutahya)	5.7	180.7	Normal	24.46	5.533
19	08.08.2019 Bozkurt (Denizli)	6	218.49	Normal	10.92	0.39
20	28.06.2020 Ege Denizi (Mugla)	5.2	214.57	Normal	61.42	3.375
21	30.10.2020 Sisam	5.1	72.95	Normal	7.71	7.056
22	21.06.2021 Aegean Sea (Datca)	5.3	228.34	Normal	14.74	0.61
23	01.10.2023 Lesvos	5	130.95	Normal	14.95	1.708
24	27.01.2024 Aegean Sea (Kusadası)	5.1	52.46	Normal	8.51	7.632
25	2.04.1996	4.9	71.81	Normal	12	18.42
26	14.11.1997 Aegean Sea (Kusadası)	5.8	128.79	Normal	12	6.03
27	09.07.1998 Aegean Sea	5	75.48	Normal	12.5	27.06
28	17.08.1999 Golcuk (Izmit)	7.6	346.5	Strike Slip	15.9	10.8
29	21.01.2002 Turgutlu (Manisa)	4.8	60.11	Normal	11.7	6.981
30	17.04.2003 Seferihisar (Izmir)	5.2	61.55	Strike Slip	11.5	8.851
31	29.01.2005	4.9	47.67	Normal	20	6.131
32	22.01.1999 Buca-İzmir	3.4	9.95	Strike Slip	5	2.985
33	24.12.2005 Akhisar (Manisa)	4.9	64.85	Normal	6	3.14

117

118

119

120



121 Table 2. GMPEs Used In this Study

NO	GROUND MOTION PREDICTION EQUATIONS
1	AS08: Abrahamson & Silva 2008 NGA Model
2	BA08: Boore & Atkinson 2008 NGA Model
3	CB08: Campbell & Bozorgnia 2008 NGA Model
4	CY08: Chiou & Youngs 2008 NGA Model
5	Abrahamson & Silva & Kamai 2014 NGA West-2 Model
6	Boore & Stewart & Seyhan & Atkinson 2014 NGA West-2 Model
7	Campbell & Bozorgnia 2014 NGA West-2 Model
8	Chiou & Youngs 2014 NGA West-2 Model

122

123 To quantify the accuracy of GMPE predictions, error analysis were conducted using statistical metrics in which
 124 the goal is to determine which GMPE provides the closest predictions to the observed data across various
 125 earthquake magnitudes and site conditions. As per the error analysis in GMPE evaluations, two methods were
 126 chosen, R² (Coefficient of Determination) and RMSE (Root Mean Square Error) and the results were given in
 127 Table 3.

128 RMSE is a commonly used metric for quantifying the difference between observed and predicted values. It
 129 measures the square root of the average of the squared differences between the predicted PGA values from GMPEs
 130 and the actual observed values. RMSE gives more weight to larger errors, making it particularly useful when larger
 131 deviations in predictions need to be minimized. RMSE can be calculated as:

132
$$RMSE = \sqrt{\frac{1}{N} \sum_{i=1}^N (PGA_{observed,i} - PGA_{predicted,i})^2}$$

133 Where:

- 134 - N is the number of the earthquake records
- 135 - PGA_{observed,i} is the observed PGA for the i-th earthquake
- 136 - PGA_{predicted,i} is the predicted PGA for the i-th earthquake based on the GMPE.

137

138

139

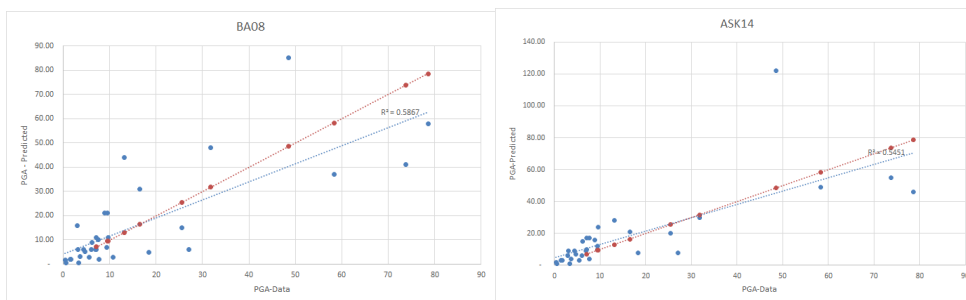
140

141

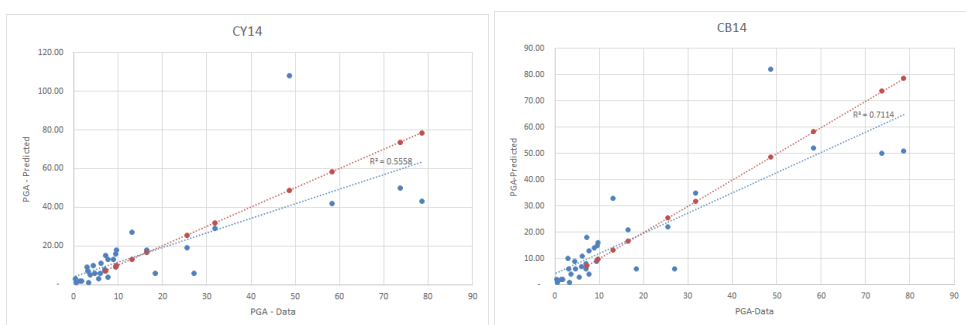
142



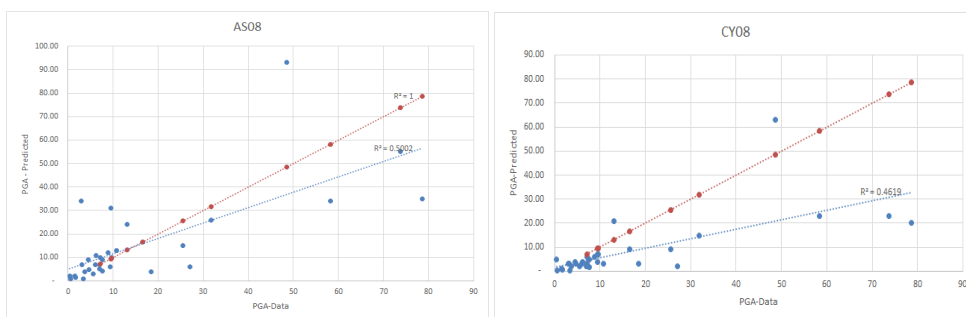
143



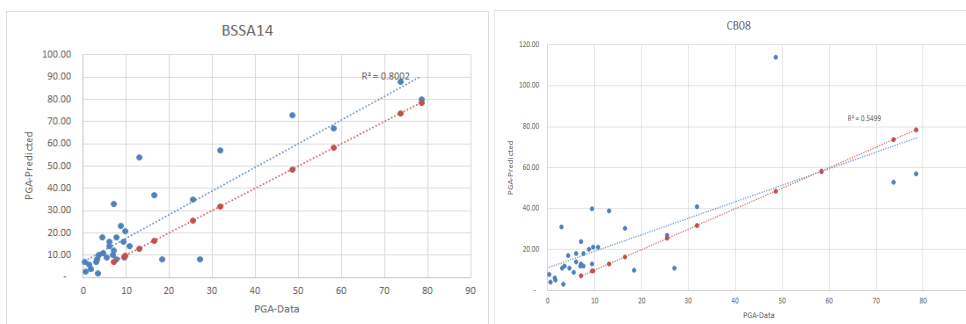
144



145



146



147 Figure 3. The results of the analysis are given in the table below.



148 Table 3. Result of GMPE Error Analysis

Root Mean Square Error							
RMSE / AS08	RMSE / BA08	RMSE / CB08	RMSE / CY08	RMSE / ASK14	RMSE / BSSA14	RMSE / CB14	RMSE / CY14
14.85	13.53	17.11	16.75	15.95	13.39	11.02	14.51
R ² (Coefficient of Determination)							
R ² / AS08	R ² / BA08	R ² / CB08	R ² / CY08	R ² / ASK14	R ² / BSSA14	R ² / CB14	R ² / CY14
0.50	0.59	0.55	0.46	0.55	0.80	0.71	0.56

149

150 There can be several factors for the observed differences between the models, for instance site and soil
 151 amplification effects or the inconsistency in depth, magnitude or distance scaling of the models and the several
 152 constants implemented in each models. As confinement of these effects and limiting the sampling data is not
 153 possible in this study, typically the error analysis is compared and the resulting ranking is used for selecting the
 154 two most powerful predictive equation. The results indicate that Model CB14 and BSSA14 are better choices for
 155 the following analysis.

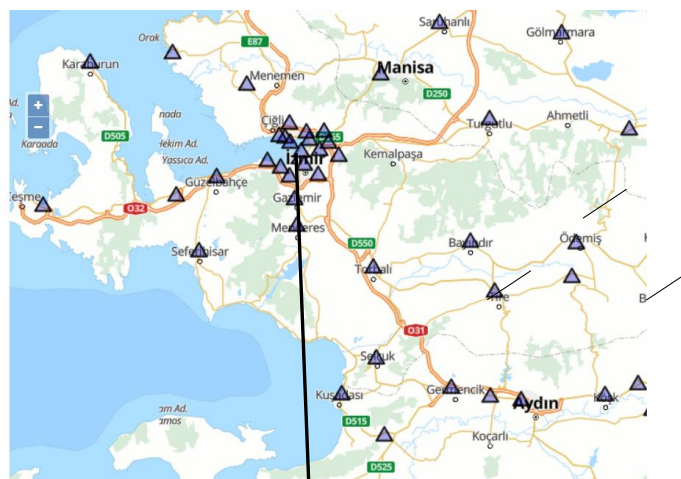
156 **3. Site response validation analysis for future predicted events**

157 The next step for the generation of future earthquakes is to evaluate and correctly determine the site properties.
 158 For that aim, 1D site response analysis (SRA) was set up and validated with the available records from 2020 Sisam
 159 earthquake. For SRA's, Deepsoil software (Hashash et.al. 2020) was used as the program was previously used by
 160 many researchers and the adaptive nature of the program was well calibrated (Cetin et.al. 2022).

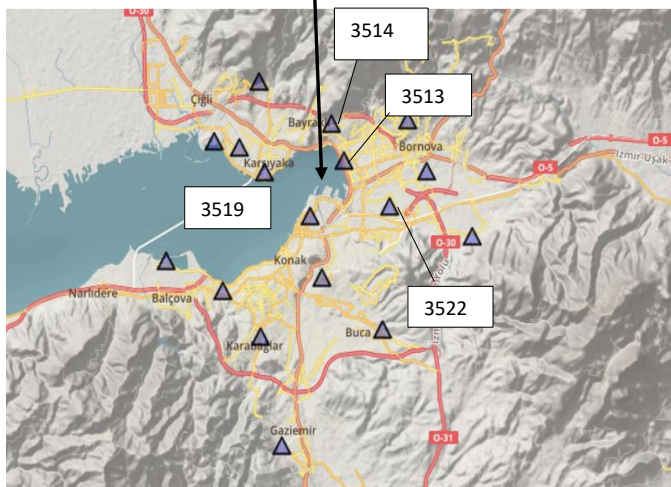
161 For calibration and validation purpose, a well recorded and data riched event was needed. The 2020 Izmir
 162 earthquake struck on October 30, 2020, with a moment magnitude (Mw) of 6.9. Its epicenter was located in the
 163 Aegean Sea, approximately 14 kilometers northeast of the Greek island of Samos, but it caused significant damage
 164 in Izmir due to its shallow depth and local site effects. Event was recorded by several seismograms located around
 165 the city (Figure 4), some of which are located on alluvial plains and some on rock outcrops, which allows
 166 researchers to further evaluate site effects (Kramer,1996). The city covers large areas of alluvial soil conditions,
 167 therefore different regions were selected for the validation purposes. One of the site is located in Karsiyaka,
 168 western part; the other sites are located in Konak- Bayrakli and Bornova.



169



170



171 Figure 4. Overview of Stations in Izmir

172 The procedure was to use and select an appropriate outcrop rock site and use its corresponding data to further
173 determine the site response analysis of the selected soil sites. The selected stations were given in Table 4, with the
174 corresponding location and PGA data's. The outcrop station was selected as station 3514, which is very close to
175 the basin area. Geotechnical and geophysical properties of the selected stations are given in Figure 5.

176

177

178

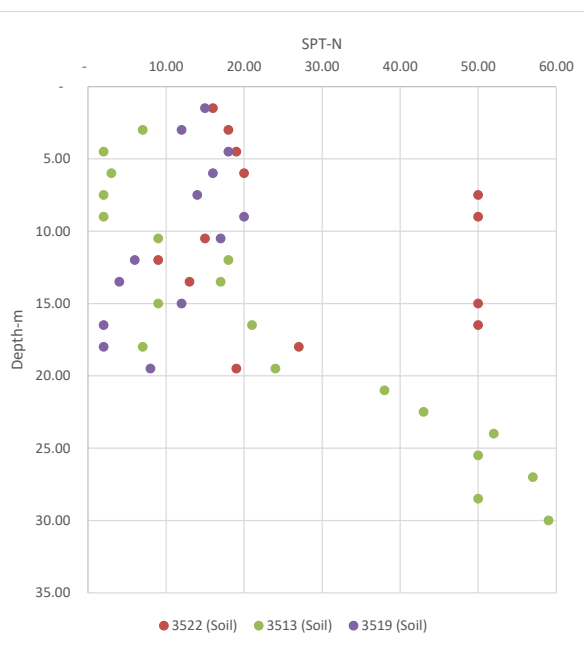
179



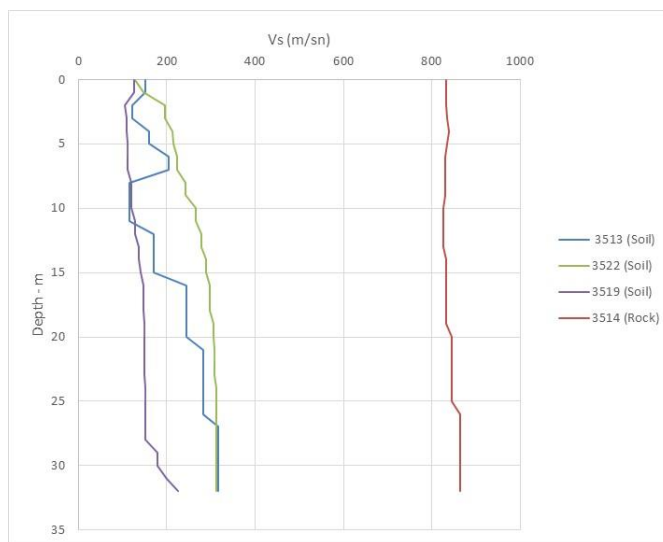
180 Table.4 Selected Soil/Rock Sites

Site Name	Region	Vs30 (m/sec)	Coordinates	PGA (g)
3514	Bayrakli	836.00	38.4762 27.1581	0.057 (E-W)
3513	Bayrakli	195.00	38.4584 27.1671	0.108 (N-S)
3519	Karsiyaka	131.00	38.4525 27.1112	0.153 (N-S)
3522	Bornova	249.00	38.4357 27.1987	0.075(E-W)

Depth/St.Name	3513 (Soil)	3522 (Soil)	3519 (Soil)
1.50		16.00	15.00
3.00	7.00	18.00	12.00
4.50	2.00	19.00	18.00
6.00	3.00	20.00	16.00
7.50	2.00	50.00	14.00
9.00	2.00	50.00	20.00
10.50	9.00	15.00	17.00
12.00	18.00	9.00	6.00
13.50	17.00	13.00	4.00
15.00	9.00	50.00	12.00
16.50	21.00	50.00	2.00
18.00	7.00	27.00	2.00
19.50	24.00	19.00	8.00
21.00	38.00		
22.50	43.00		
24.00	52.00		
25.50	50.00		
27.00	57.00		
28.50	50.00		
30.00	59.00		
31.50			
33.00			
34.50	SOIL TYPE DESCRIPTION INDEX (PER ASTM)		
36.00	CL/CH		
37.50			
39.00	SM		
40.50			
42.00	SC		
43.50			
45.00	GM		
46.50			
48.00	GC		
49.50			



181

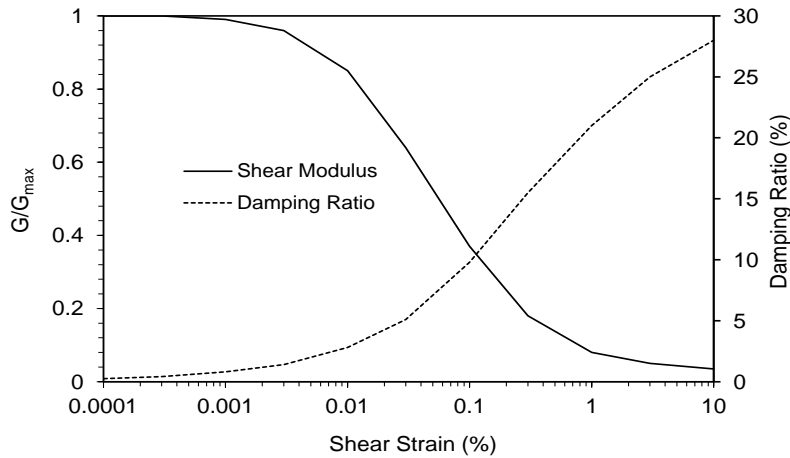


182

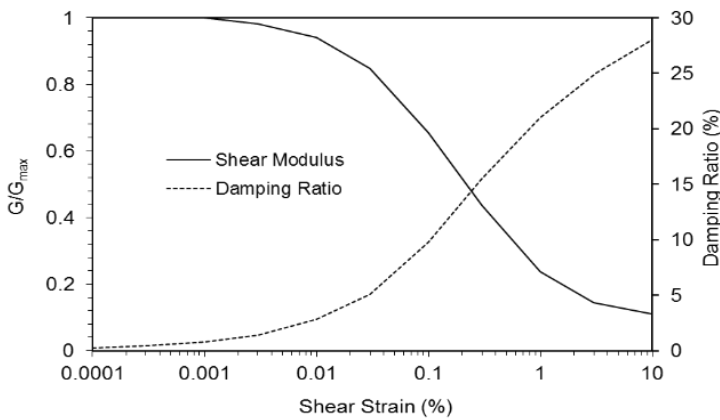
183 Figure 5. Geotechnical / Geophysical properties of the selected rock / soil stations

184 Detailed soil profiles and parameters were gathered from available deeper site profiles and deep geophysical
185 measurements that were used from the wide range of database. (Cetin et al, 2022) The modulus reduction and
186 damping curves were used from the literature by adopting soil parameters and the general trend of the curves were
187 given in Figure 6.

188 The results of the analysis were given for 3 different locations in the city center as previously stated. The motivation
189 for selecting 3 different regions was to take into account of different soil/geophysical properties of soils which
190 have alluvial soil deposits. The second motivation come from the fact that, to be able to generate a general response
191 spectrum, a more representative solution should be taken into account which represents the different soil conditions
192 and regions of the city (Figure 7-8-9).



193



194

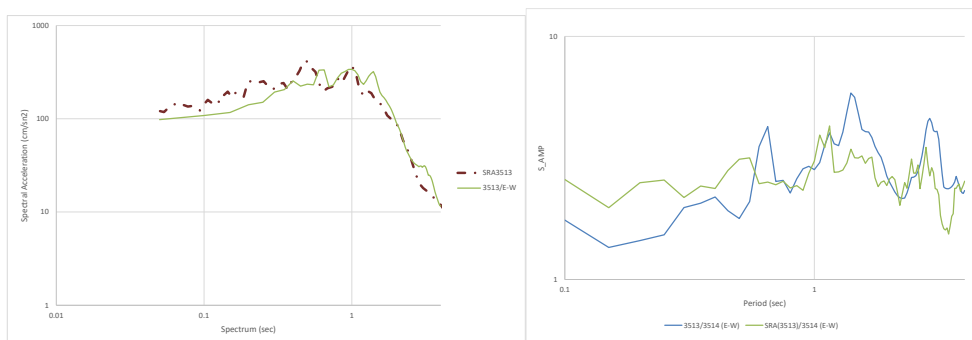
195 Figure 6. Modulus Reduction/Damping Curves for Sandy-Cohesionless Soils (Seed and Idriss, 1970) and
196 Cohesive Type Soils (Vucetic-Dobry, 1991)

197 In the results, comparison of the response spectrum graphs of SRA with the recorded site motion and corresponding
198 amplification function $S_{amp} = SR(\text{site}) / SR(\text{outcrop})$ were given for the 3 selected stations. It can be seen that
199 the 3513 station amplifications increased up to 4 - 4.5 times in 1.50 s periods. Similar to 3513 station, at 3522
200 Bornova station, amplifications were observed for the same period region with 3.0 – 3.5 times increase. These
201 two regions were close to each other and the geotechnical site conditions were similar to each other compared to
202 the Karsiyaka station. When the outcomes of Karsiyaka station (3519) was examined, similar amplification data
203 was obtained but in higher period regions, 2.50 seconds and later.

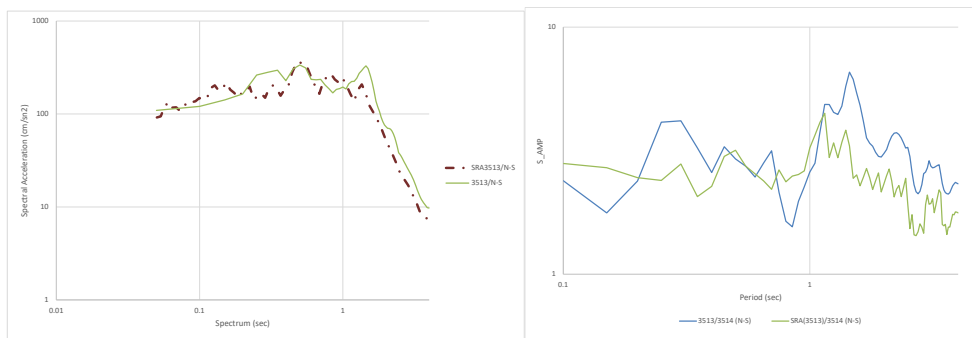
204



205



206



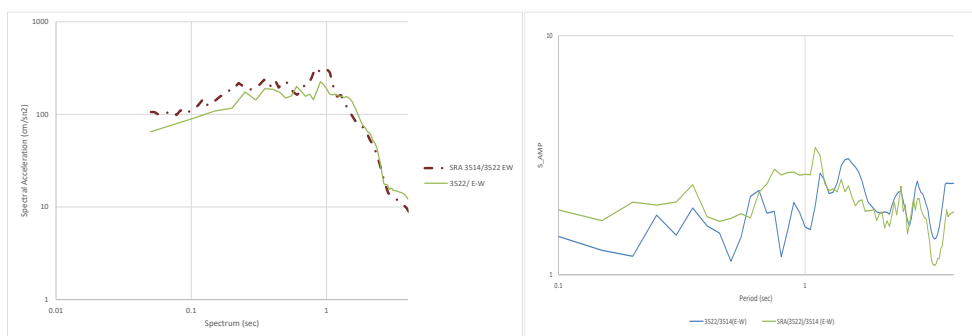
207

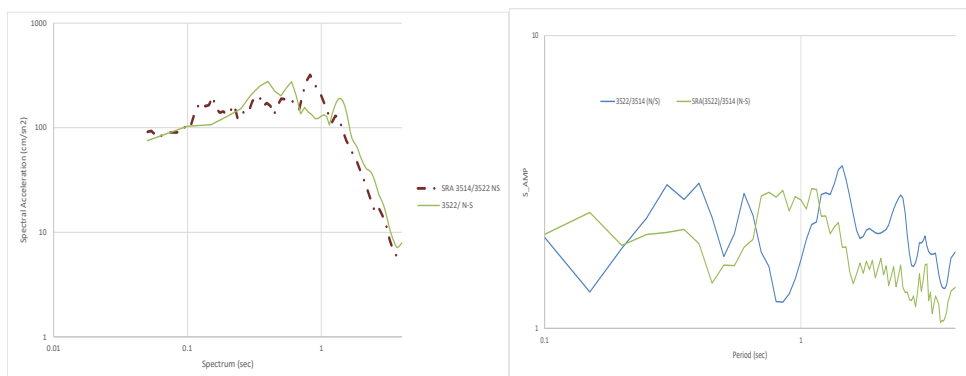
Figure 7. The comparison of recorded and estimated (SRA) elastic response and amplification spectra for 2020

208

Samos event@station 3513

209

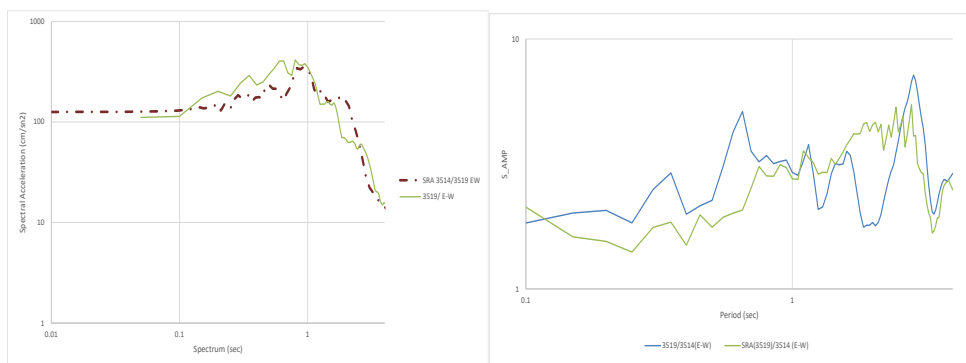




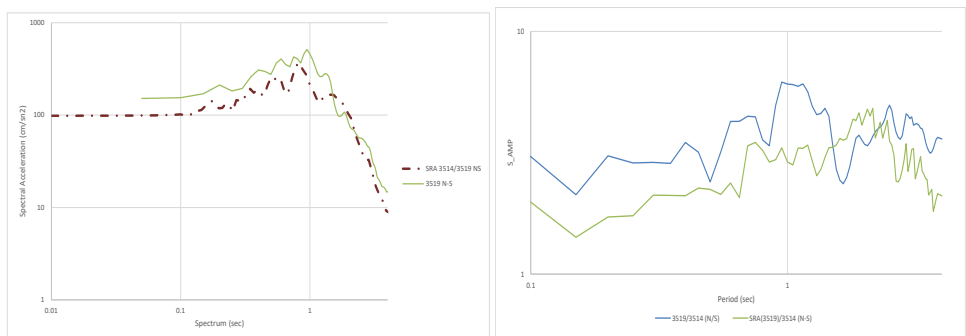
210

211 Figure 8. The comparison of recorded and estimated (SRA) elastic response and amplification spectra for 2020

212 Samos event@station 3522



213



214

215 Figure 9. The comparison of recorded and estimated (SRA) elastic response and amplification spectra for 2020

216 Samos event@station 3519

217



218 The results indicate a conformity in the general trend of spectrum and have been found to be consistent with the
219 actual data especially in the period range of 0.50-1.50 sec range which coincides with the general building stock
220 (6-10 story heights) of the city. Overall, it can be concluded that, in most instances, the average spectra of the
221 recorded motions fall within the range of those associated with the calculated motions. The match between the
222 75th percentile of the recorded motions and the computed motions varies from moderate to very good. Similar
223 results can also be seen in Cetin et.al. (2024).

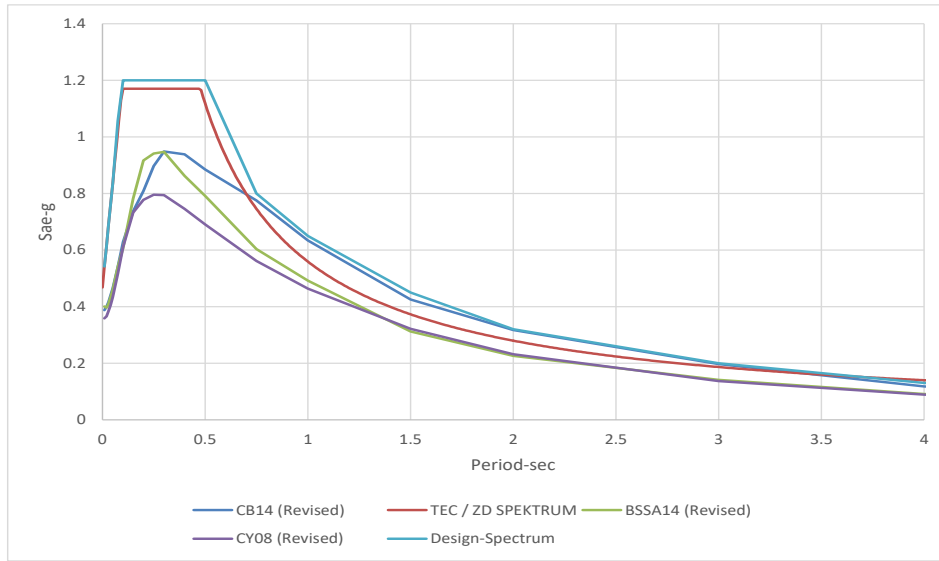
224 By evaluating the data and analysis results obtained so far, a reasonably usable SRA model and GMPE
225 relationships that can correspond to the seismicity of the general region have been revealed. The next stage will
226 be selecting the target spectrum for possible future earthquakes and then determining the spectral outcomes for
227 selected regions by performing SRA analyzes.

228 **4. Selecting target response spectrum and evaluating the results of future events**

229 Using the most appropriate GMPE identified through the error analysis as stated before, ground motion parameters
230 such as Peak Ground Acceleration (PGA), Spectral Acceleration (SA), and others are predicted for a future
231 predicted deterministic scenario conditions. The target spectrum was generated for the deterministic scenario of
232 Radius Project (Radius, 1997) which was a detailed study for the seismicity of the region. The Project concluded
233 with a deterministic scenario which include an Mw 6.5 event in Izmir fault with an anticipated distance of 4 km.

234 An important consideration in site-specific seismic hazard analyses is the near-fault effect and the maximum
235 directional effect. Somerville et al. (1997) adjusted empirical ground motion attenuation models to account for the
236 influence of rupture directivity on both amplitude and duration. Rupture directivity happens when seismic energy
237 is concentrated along the path of fault rupture, leading to a substantial increase in ground motions in that direction.
238 This phenomenon is particularly significant for sites near faults, where rupture directivity can cause ground
239 motions to be considerably stronger in one direction, especially at longer periods, compared to others. This
240 behaviour can be observed in 2000 Samos event after investigating the N-S and E-W spectrums. The directivity
241 of the fault enhance the motions in N-S directions, which can also be associated with the damage behaviour of
242 buildings in Mavisehir- Karsiyaka region, specifically at station 3519. Therefore, this effect has been considered
243 in future earthquake simulations as well and the selected GMPE were revised accordingly. Target spectrum was
244 selected taking into account that the TEC and GMPE spectrums will not be underscored at ant period point.
245 Therefore, a new spectrum is generated which takes into account of the historical seismicity of the region as well
246 as the current regulations (Figure 10).

247



248

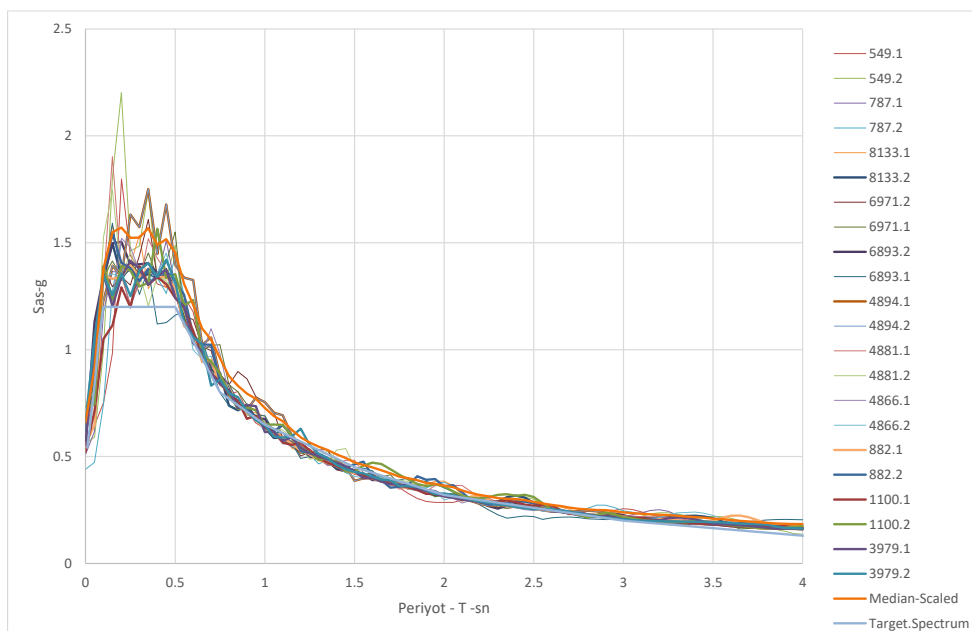
249 Figure 10. Design Spectrum for the site with comparisons

250 There are a total of 11 records were selected (Table 5) and scaled to the given target spectrum (Figure 11). The
 251 scaling of the records are generated through Seismosoft software. The results of the selected and scaled ground
 252 motions are given together in Figure 11.

253 Table 5. Selected Ground Motion Records

No	Record Sequence Number	Scale Factor	Earthquake Name	Year	Station Name	Magnitude	Mechanism	Rjb (km)	Rrup (km)	Vs30 (m/sec)
1	4881	2.32	"Chuetsu-oki_Japan"	2007	"Nagaoka Kouiti Town"	6.8	Reverse	11.61	20.77	294.38
2	549	1.91	"Chalfant Valley-02"	1986	"Bishop - LADWP South St"	6.19	strike slip	14.38	17.17	303.47
3	6893	1.07	"Darfield_New Zealand"	2010	"DFHS"	7	strike slip	11.86	11.86	344.02
4	8133	4.31	"Christchurch_New Zealand"	2011	"SLRC"	6.2	Reverse Oblique	31.81	31.81	249.28
5	6971	2.12	"Darfield_New Zealand"	2010	"SPFS"	7.0	strike slip	29.86	29.86	389.54
6	882	2.57	"Landers"	1992	"Desert Hot Springs"	7.28	strike slip	26.84	26.84	344.67
7	4866	1.26	"Chuetsu-oki_Japan"	2007	"Kawanishi Izumozaki"	6.8	Reverse	0.0	11.75	338.32
8	4894	0.38	"Chuetsu-oki_Japan"	2007	"Kashiwazaki NPP_Unit 1: ground surface"	6.8	Reverse	0.0	10.97	329.0
9	787	1.43	"Loma Prieta"	1989	"Palo Alto - SLAC Lab"	6.93	Reverse Oblique	30.62	30.86	425.3
10	1100	2.03	"Kobe_Japan"	1995	"Abeno"	6.9	strike slip	24.85	24.85	256.0
11	3979	2.82	"San Simeon_CA"	2003	"Cambria - Hwy 1 Caltrans Bridge"	6.52	Reverse	6.97	7.25	362.42

254

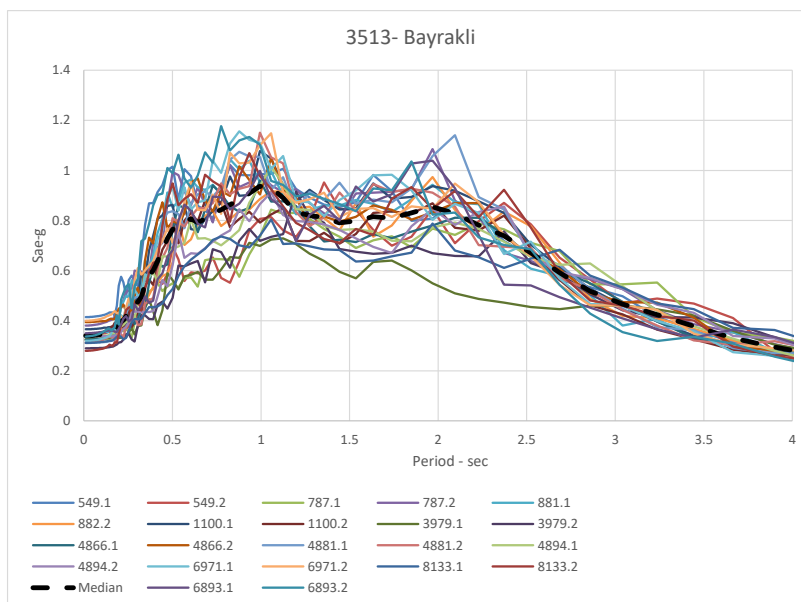


255

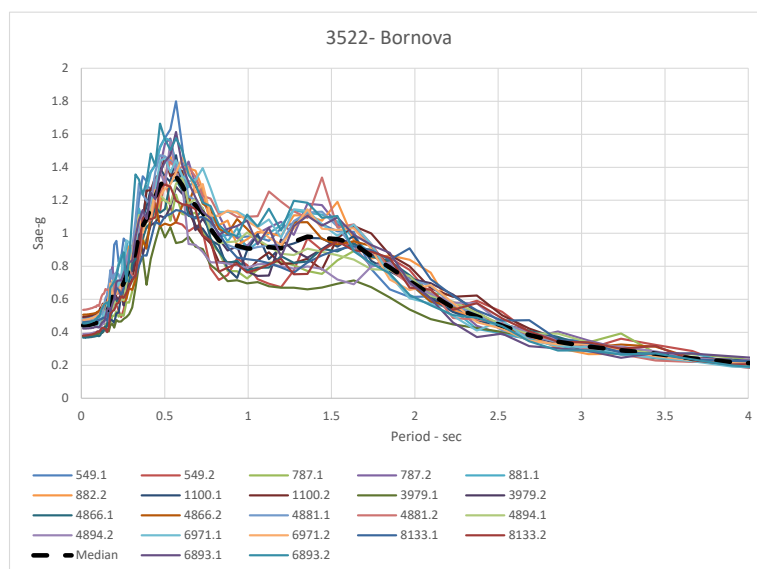
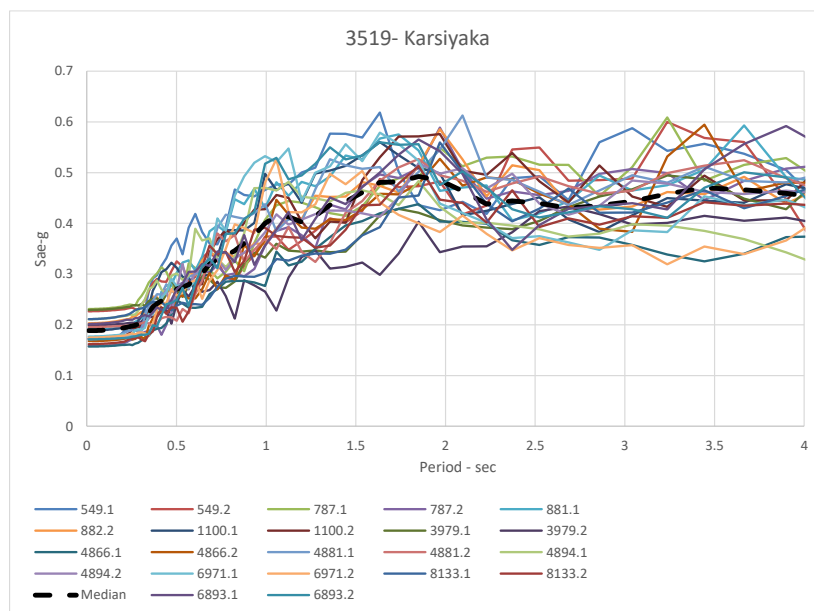
256 Figure 11. Selected and Scaled Ground Motion with respect to target spectrum

257 Using the deepsoil model calibrated in previous sections, site-specific earthquake analyzes with selected records

258 were carried out for each region/station and results were given in Figure 12.



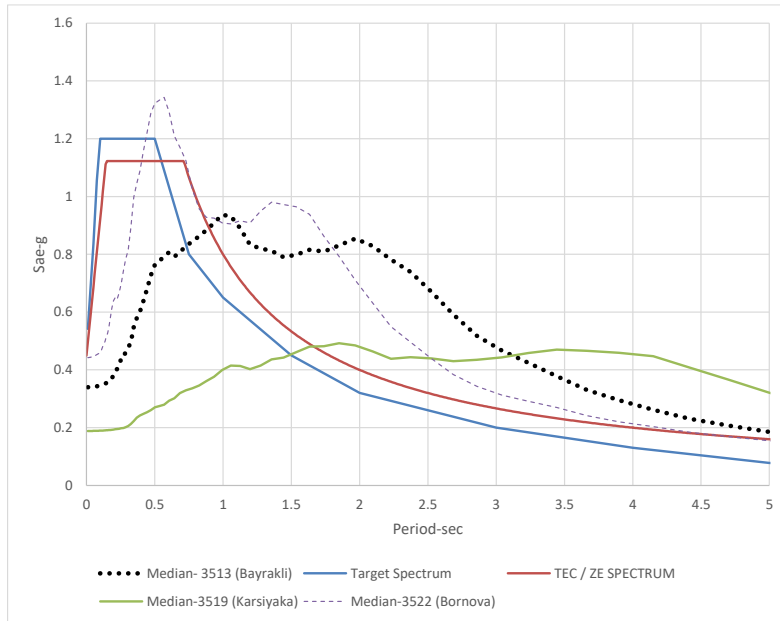
259



261

262 Figure 12. Outcome of the future anticipated scenario earthquake in the city with 3 different regions (Bayrakli,
263 Karsiyaka and Bornova)

264 The comparison of each region with the current TEC and target spectrum were given in Figure 13.



265

266 Figure 13. The comparison of stations with the current TEC and target spectrum

267 According to TEC, local site effects are taken into account by some modification factors. These modification
 268 factors are called F_1 and F_S values and defined by the following relationship:

269 $S_{ds} = S_S F_S$ (S_{ds} = Design Spectral Acceleration Value for short period region)

270 $S_{d1} = S_1 F_1$ (S_{d1} = Design Spectral Acceleration Value for 1sec period region)

271 Where S_S and S_1 are the spectral values without taking into account the local site effects.

272 The result of the analysis showed that the local site modification factors should be corrected by at least two times
 273 as summarized in Table 6.

274 Table 6. Local site modification factors (F_1) according to TEC and SAR of scenario earthquake

Station	Vs30	Soil Class (Acc TEC)	F1/ TEC	F1/ SAR, t=1 sec
3513	195	ZD	2.054	4.21
3522	249	ZD	2.054	4.76
3519	131	ZE	2.935	4.40

275

276

277

278

279



280 **5. Summary and Conclusions**

281 In this study, based on the past seismicity of the city of Izmir, potential future seismicity of the city of city has
282 been considered and various analyses have been conducted. A summary of these studies is provided below.

- 283 - Firstly, using a dataset of past recorded earthquake events, the level of agreement with current GMPE
284 equations was investigated. Based on the evaluations, two GMPEs were selected for use in determining
285 target spectrum parameters for site-specific seismicity analysis.
- 286 - To perform site-specific seismic analyses, well-recorded event of İzmir-Samos earthquake data were
287 utilized. A 1D analysis model, using the available geotechnical data was applied for 3 different stations.
288 These stations were selected for the aim to
- 289 ○ represent different alluvial soil conditions of the city
 - 290 ○ take in to account of the 3 most populated, therefore representative regions of the city
 - 291 ○ be able to arrive a more general conclusion about the possible future earthquake simulations
- 292 - Future potential earthquake scenarios have been selected. For this purpose, a target spectrum was
293 developed for an $M_w=6.5$ earthquake on the İzmir fault, as part of the RADIUS 2005 project. The
294 resulting target spectrum was modified to account for near-field and directivity effects and subsequently
295 used in the analyses.
- 296 ○ The TEC was also utilized in the selection of the target spectrum. Ultimately, the chosen target
297 spectrum was developed to satisfy both deterministic and probabilistic approaches given by the
298 code recommendations.
- 299 - Eleven earthquake records were selected and scaled to match the target spectrum. Subsequently, using
300 the same validated models, possible scenario earthquake outcomes were analyzed.

301 The results obtained from the analyses are provided below:

- 302 - The 2020 Samos earthquake has been a significant event for site-specific seismicity studies due to the
303 abundance of recording stations and the rich data content available. In the analyses conducted,
304 amplifications were observed in the high-period region.
- 305 - GMPEs were evaluated and compared using the past seismic activity of the city. That further allow to
306 generate a target spectrum for the city.
- 307 - While generating a target spectrum, particularly when considering near-field effects and directivity
308 effects, the obtained spectra possess a broader energy content than those presented in the regulations. This
309 condition should be taken into account in seismic design codes.
- 310 - The acceleration spectra obtained at the surface are amplified by at least a factor of 2 for periods of 1
311 second and longer. More specifically, the result of the analysis showed that the local site modification
312 factors defined by TEC should be corrected by at least 2.50 times. This condition should be taken into
313 account in all of the alluvial regions of the city especially when designing more than 8-10 stories of
314 buildings.
- 315 - Different regions selected in this study provides a framework for a future study which will emphasize on
316 the basin effect discussed in other papers.



317 **Funding** The authors declare that no funds, grants, or other support were received during the preparation of his
318 manuscript.

319 **Data availability** all data and models analyzed during the current study are available from the corresponding
320 author on reasonable request.

321 **Declarations**

322 **Competing interests** the authors have no relevant financial or non-financial interests to disclosure.

323 6. References

324 Abrahamson NA, Silva W. Summary of the Abrahamson & Silva NGA groundmotion relations. *Earthq Spectra*
325 2008;24:67–97. <https://doi.org/10.1193/1.2924360>

326 Abrahamson NA, Silva WJ, Kamai R. Summary of the ASK14 ground motion relation for active crustal regions.
327 *Earthq Spectra* 2014;30:1025–55. <https://doi.org/10.1193/070913EQS198M>

328 Boore DM, Atkinson GM (2008) Ground-motion prediction equations for the average horizontal component of
329 PGA, PGV, and 5%-damped PSA at spectral periods between 0.01 s and 10.0 s. *Earthq Spectra* 24:99–138.
330 <https://doi.org/10.1193/1.2830434>

331 Boore DM, Stewart JP, Seyhan E, Atkinson GM. NGA-West2 equations for predicting PGA, PGV, and 5%
332 damped PSA for shallow crustal earthquakes. *Earthq Spectra* 2014;30:1057–85.
333 <https://doi.org/10.1193/070113EQS184M>

334 Campbell KW, Bozorgnia Y. NGA ground motion model for the geometric mean horizontal component of PGA,
335 PGV, PGD and 5% damped linear elastic response spectra for periods ranging from 0.01 to 10 s. *Earthq Spectra*
336 2008;24:139–71. <https://doi.org/10.1193/1.2857546>

337 Campbell KW, Bozorgnia Y. NGA-West2 ground motion model for the average horizontal components of PGA,
338 PGV, and 5% damped linear acceleration response spectra. *Earthq Spectra* 2014;30:1087–115.
339 <https://doi.org/10.1193/062913EQS175M>.

340 Cetin, K.O., Cakir, E. & Zazour, M. Seismic site effect models for the Turkiye-Izmir-Bayrakli Basin. *Bull*
341 *Earthquake Eng* 22, 303–328 (2024). <https://doi.org/10.1007/s10518-023-01774-z>

342 Chiou, B.S.J. and Youngs, R.R. (2008) An NGA Model for the Average Horizontal Component of Peak Ground
343 Motion and Response Spectra. *Earthquake Spectra*, 24, 173-215. <https://doi.org/10.1193/1.2894832>

344 Chiou BSJ, Youngs RR. Update of the Chiou and Youngs NGA model for the average horizontal component of
345 peak ground motion and response spectra. *Earthq Spectra* 2014;30:1117–53.
346 <https://doi.org/10.1193/072813EQS219M>

347 Dan McKenzie, Active tectonics of the Alpine—Himalayan belt: the Aegean Sea and surrounding
348 regions, *Geophysical Journal International*, Volume 55, Issue 1, October 1978, Pages 217–
349 254, <https://doi.org/10.1111/j.1365-246X.1978.tb04759.x>

350 Emre, Ö., Duman, T.Y., Özalp, S. *et al.* Active fault database of Turkey. *Bull Earthquake Eng* **16**, 3229–3275
351 (2018). <https://doi.org/10.1007/s10518-016-0041-2>

352 Emre O, Ozalp S, Dogan A, Ozaksoy V, Yildirim C, Goktas F (2005) Active faults in the vicinity of Izmir and
353 their earthquake potentials [in Turkish], Report No: 10754, Geological Studies Department, General Directorate
354 of Mineral Research and Exploration, Ankara, Turkey

355 Hashash YMA, Musgrove MI, Harmon JA, Ilhan O, Xing G, Numanoglu O. DEEPSOIL V7.0, User manual.
356 Urbana, IL: Board of Trustees of University of Illinois at Urbana-Champaign; 2020



- 357 Kemal Onder Cetin, Selim Altun, Aysegul Askan, Mustafa Akgün, Alper Sezer, Cem Kınca, et.al., The site effects
358 in Izmir Bay of October 30 2020, M7.0 Samos Earthquake, Soil Dynamics and Earthquake Engineering, Volume
359 152, 2022, 107051, ISSN 0267-7261, <https://doi.org/10.1016/j.soildyn.2021.107051>.
- 360 Kramer SL (1996) Geotechnical earthquake engineering, Prentice Hall, Upper Saddle River
- 361 Neslihan Ocakoğlu, Emin Demirbağ, İsmail Kuşçu, Neotectonic structures in İzmir Gulf and surrounding regions
362 (western Turkey): Evidences of strike-slip faulting with compression in the Aegean extensional regime, Marine
363 Geology, Volume 219, Issues 2–3, 2005, Pages 155-171, ISSN 0025-3227,
364 <https://doi.org/10.1016/j.margeo.2005.06.004>.
- 365 Nihal Akyol, Lupei Zhu, Brian J. Mitchell, Hasan Sözbilir, Kıvanç Kekovalı, Crustal structure and local seismicity
366 in western Anatolia, *Geophysical Journal International*, Volume 166, Issue 3, September 2006, Pages 1259–
367 1269, <https://doi.org/10.1111/j.1365-246X.2006.03053.x>
- 368 Paul G. Somerville, Nancy F. Smith, Robert W. Graves, Norman A. Abrahamson; Modification of Empirical
369 Strong Ground Motion Attenuation Relations to Include the Amplitude and Duration Effects of Rupture
370 Directivity. *Seismological Research Letters* 1997;; 68 (1): 199–222. doi: <https://doi.org/10.1785/gssrl.68.1.199>
- 371 RADIUS (1997), Risk assessment tools for diagnosis of urban areas against seismic disaster Izmir earthquake
372 master program, Bogazici University Kandilli Observatory, Istanbul, Turkey
- 373 Seed, H. B., and Idriss, I. M. (1970). "Soil moduli and damping factors for dynamic response analyses," Report
374 No. EERC 70-10, Earthquake Engineering Research Center, Univ. of California, Berkeley, California. Berkeley,
375 December.
- 376 Seismomatch, Software by Seismosoft
- 377 Tepe, Çiğdem; Sözbilir, Hasan; Eski, Semih; Sümer, Ökmen; And Özkaymak, Çağlar (2021) "Updated historical
378 earthquake catalog of İzmir region (western Anatolia) and its importance for the determination of seismogenic
379 source," *Turkish Journal of Earth Sciences*: Vol. 30: No. 8, Article 6. <https://doi.org/10.3906/yer-2101-14>
- 380 Turkish Building Earthquake Code. TEC); 2018
- 381 Turkish Ministry of Interior Disaster and Emergency Management Presidency (AFAD), Ankara, Türkiye,
382 <https://tadas.afad.gov.tr>
- 383 Vucetic, M. and Dobry, R. (1991) Effect of Soil Plasticity on Cyclic Response. *Journal of Geotechnical*
384 *Engineering*, 117, 89-107. [http://dx.doi.org/10.1061/\(ASCE\)0733-9410\(1991\)117:1\(89\)](http://dx.doi.org/10.1061/(ASCE)0733-9410(1991)117:1(89))
- 385 Zeynep Gülerce , Burak Akbas., A. Arda Ozacar , Eyüp Sopacı, Fatih M. Onder , Bora et.al. "Predictive
386 performance of current ground motion models for recorded
387 strong motions in 2020 Samos Earthquake" *Soil Dynamics and Earthquake Engineering* 152 (2022) 107053